Heliyon 8 (2022) e09029

Contents lists available at ScienceDirect

Heliyon

journal homepage: www.cell.com/heliyon

Research article

SIAH ubiquitin E3 ligases as modulators of inflammatory gene expression

M. Lienhard Schmitz [a,1], Jan Dreute [a,1], Maximilian Pfisterer [a,1], Stefan Günther [b], Michael Kracht [c], Shashipavan Chillappagari [a,*]

[a] Institute of Biochemistry, Justus-Liebig-University, D-35392, Giessen, Germany
[b] Bioinformatics and Deep Sequencing Platform, Max Planck Institute for Heart and Lung Research, D-61231, Bad Nauheim, Germany
[c] Rudolf-Buchheim-Institute of Pharmacology, Justus-Liebig-University, D-35392, Giessen, Germany

HIGHLIGHTS

- SIAH1/2 function as modulators of IL-1α-triggered gene expression.
- SIAH1/2 do not participate in the activation of the canonical NF-κB pathway.
- SIAH1/2 control the stability of the coactivator p300.

ARTICLE INFO

Keywords:
SIAH1
SIAH2
Ubiquitin E3 ligase
NF-κB
Inflammatory gene expression

ABSTRACT

The functionally redundant ubiquitin E3 ligases SIAH1 and SIAH2 have been implicated in the regulation of metabolism and the hypoxic response, while their role in other signal-mediated processes such inflammatory gene expression remains to be defined. Here we have downregulated the expression of both SIAH proteins with specific siRNAs and investigated the functional consequences for IL-1α-induced gene expression. The knockdown of SIAH1/2 modulated the expression of approximately one third of IL-1α-regulated genes. These effects were not due to changes in the NF-κB and MAPK signaling pathways and rather employed further processes including those mediated by the coactivator p300. Most of the proteins encoded by SIAH1/2-regulated genes form a regulatory network of proinflammatory factors. Thus SIAH1/2 proteins function as variable rheostats that control the amplitude rather than the principal activation of the inflammatory gene response.

1. Introduction

The mammalian family of SIAH (seven-in-absentia) ubiquitin E3 ligases contains three orthologues: SIAH1, SIAH2 and SIAH3 [1] Only SIAH1 and SIAH2 contain a functional RING finger required for their E3 ligase activity, suggesting that SIAH3 is an enzymatically inactive variant [1]. SIAH1 and SIAH2 catalyze the attachment of K48-linked (poly)ubiquitin chains as well as mono- or di-ubiquitination [2]. SIAH1 and SIAH2 can homo- and heterodimerize, providing a plausible explanation for the finding that they have been found to execute distinct and also overlapping functions. This is also reflected by genetic models, as *Siah2*$^{-/-}$ deficient mice are viable, while the additional deletion of the *Siah1a* allele (mice have 2 different SIAH1 forms) causes neonatal death [3]. There is convincing evidence for a role of SIAH1 and SIAH2 in the regulation of cell metabolism and the hypoxic response [4, 5, 6]. In contrast, their potential functions in the innate immune response are not clear. A role of SIAH proteins for innate immune signaling has been proposed by studies based on their ability to bind several different viral proteins including the Herpes simplex virus (HSV)-encoded immediate-early protein ICP0 [7], the Dengue virus (DENV)-encoded non-structural protein 5 (NS5) [8] and the Hepatitis B virus X protein [9]. In addition, SIAH1 has been found to associate with various proteins with relevance in innate immune signaling including the adapter protein MYD88D [10], XIAP [11] and TRIM8 [12]. Overexpression experiments and reporter gene assays suggested a supportive role of SIAH1 for activation of the proinflammatory transcription factor NF-κB [13]. Activation of this transcription factor is initiated by a cytosolic response where signaling cascades lead to the decay of inhibitory IκB proteins followed by the generation of free DNA-binding dimers, while a second level of

* Corresponding author.
E-mail address: Shashi.Chillappagari@biochemie.med.uni-giessen.de (S. Chillappagari).
[1] These authors contributed equally to this work.

https://doi.org/10.1016/j.heliyon.2022.e09029
Received 31 August 2021; Received in revised form 19 December 2021; Accepted 24 February 2022

regulation in the nucleus mediates the precise control of target gene specificity and all parameters of NF-κB-driven gene expression [14]. In contrast to the NF-κB activating function of SIAH1, the analysis of *Siah2*$^{-/-}$ animals did not reveal changes in TNFα-induced cytosolic signaling pathways [3]. This lack of phenotype might be due to the known compensatory activity of SIAH1 [3], suggesting that only the simultaneous deletion of SIAH1 and SIAH2 can clarify their potential role in inflammation.

2. Results and discussion

As the simultaneous deletion of *Siah2* and *Siah1a* genes is embryonically lethal [3], we decided to study the role of SIAH1 and SIAH2 by simultaneous knockdown of both E3 ligases with specific siRNAs in human cells. In a first step we downregulated SIAH1 and SIAH2 either alone or in combination with specific siRNAs in HeLa epithelial cells, which are a widely used model to study innate immune signaling [15].

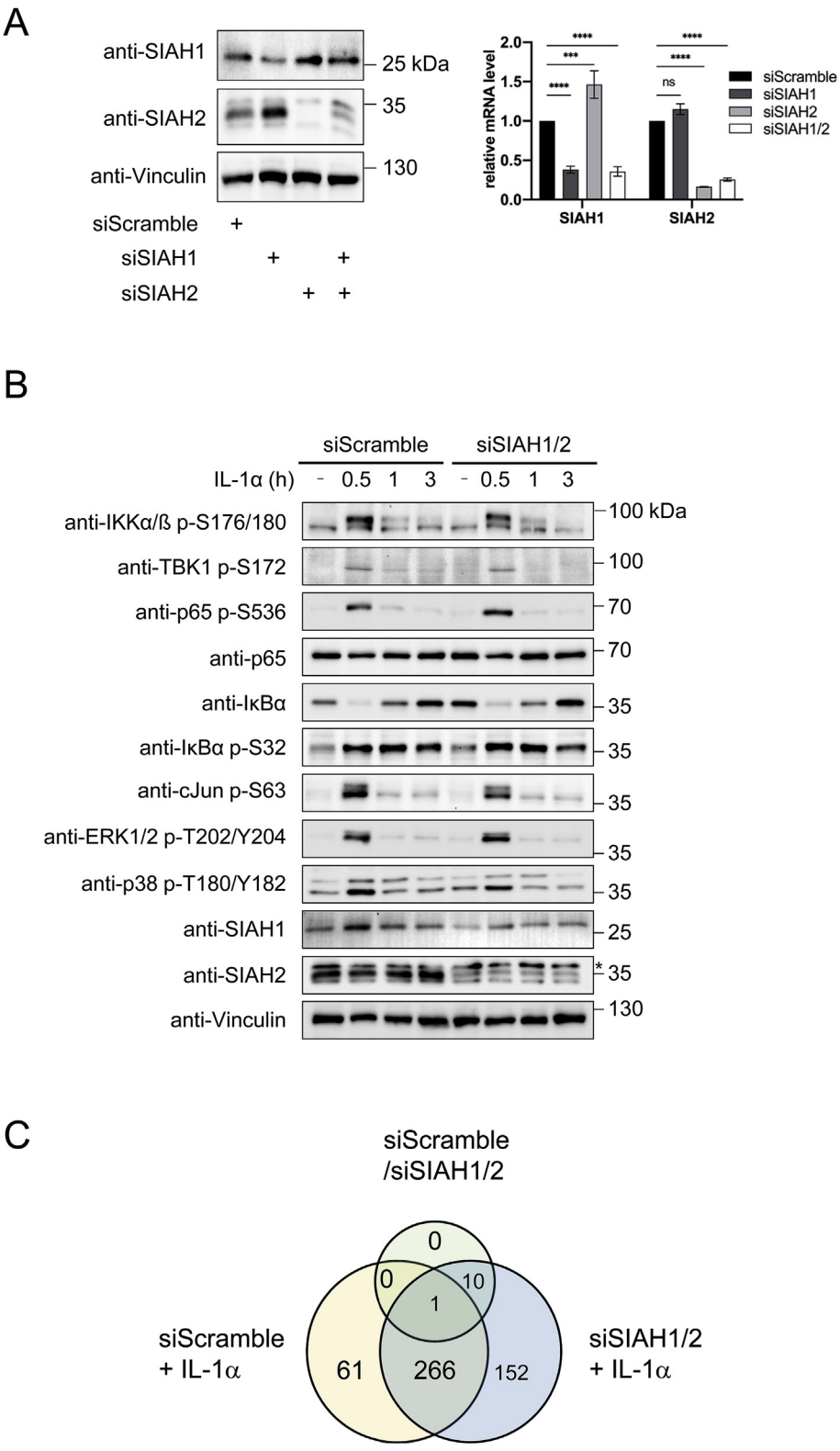

Figure 1. Regulation of inflammatory signaling and gene expression by SIAH1/2. (A) HeLa cells were treated with siRNAs targeting SIAH1 and/or SIAH2 or an adequate scrambled control as shown. After two days cells were harvested and analyzed either by Western blotting (left) or RT-qPCR (right), error bars show standard deviations. Asterisks indicate *P*-values (***p ≤ 0.001, ****p ≤ 0.0001) obtained by two-way ANOVA, ns = not significant. (B) HeLa cells were transfected with the indicated siRNAs. Two days later cells were treated with IL-1α for the indicated periods and protein extracts were analyzed for the expression and phosphorylation of the signaling proteins as shown. The positions of molecular weight markers are indicated, non-specific signals are indicated by an asterisk. (C) HeLa cells were treated with SIAH1/2-specific siRNAs or scrambled controls and two days later stimulated for 4 h with IL-1α (10 ng/ml), followed by RNA-seq analysis. Genes with >1,5-fold regulation and FDR<0.05 were used for visualization in the Venn diagram.

While SIAH1-specific siRNAs caused an incomplete reduction at the mRNA and protein levels of this protein, they also led to a compensatory upregulation of SIAH2, which was evident at the protein level but not at the mRNA level (Figure 1A). Similarly, also knockdown of SIAH2 caused a slight increase of *Siah1* mRNA and protein, consistent with the concept of mutual functional compensation of both ligases. As mentioned above, this idea is supported by genetic data showing lethality of the combined knockout [3] and biochemical data revealing the ability to heterodimerize [16].

In order to test the effect of combined SIAH1 and SIAH2 knockdown on inflammatory signaling cascades, cells were exposed to the cytokine IL-1α for various periods reflecting the induction and termination phase of inflammatory signaling. Western blot experiments were performed with specific antibodies determining the amount and phosphorylation status of key signaling intermediates. These experiments showed no significant impact of SIAH1/2 knockdown on NF-κB signaling, as revealed by similar kinetics of IL-1α-induced decay and re-synthesis of IκBα and also by comparable phosphorylations of p65 and its upstream kinases (Figure 1B). Similarly, activation of proinflammatory mitogen-activated protein kinases (MAPKs) was comparable between controls and SIAH1/2 knockdown cells, as revealed by Western blotting and their quantitative analysis (Figure 1B and suppl. Figure 1).

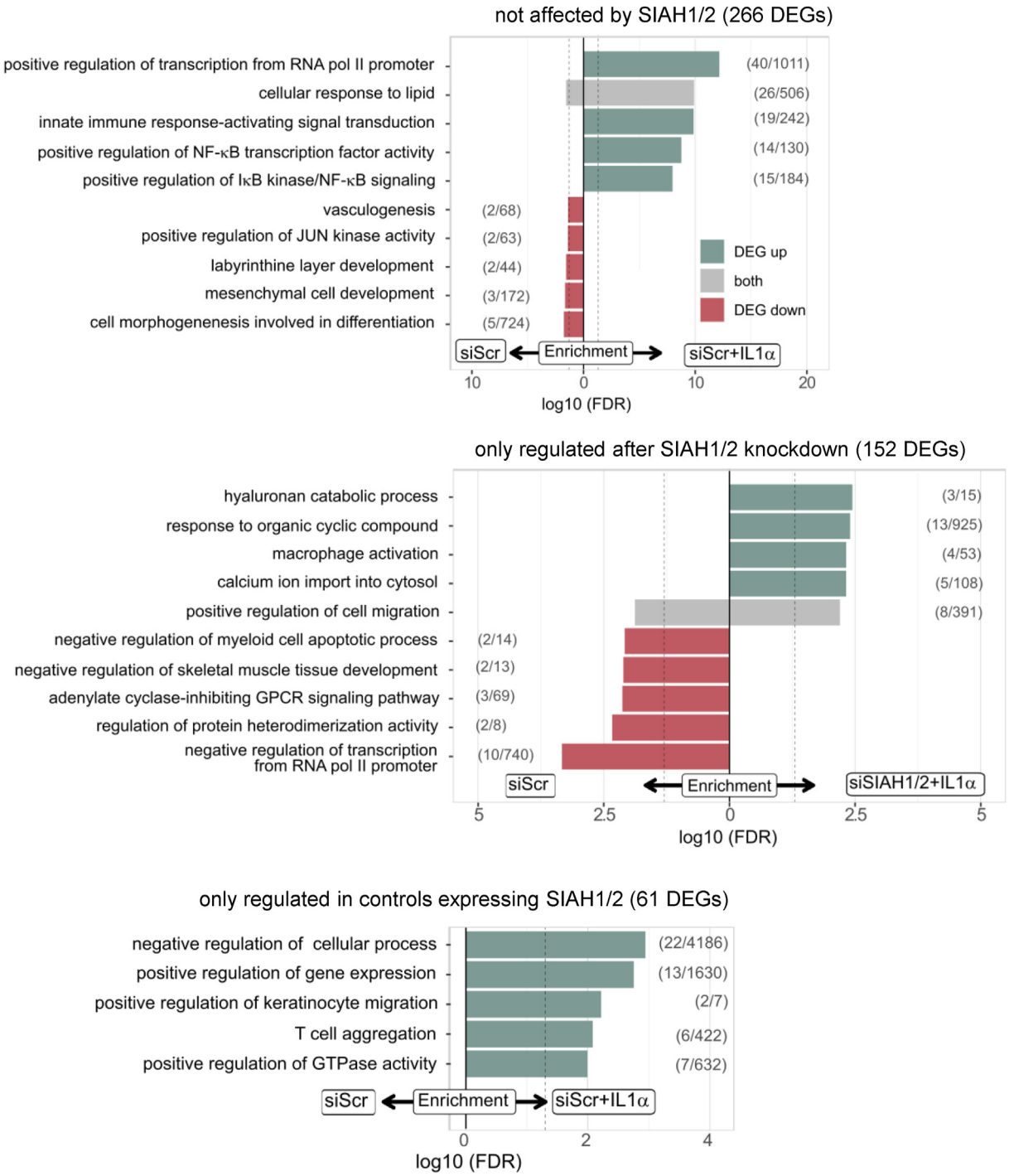

Figure 2. GO analysis of IL-1α-regulated genes. The three groups of genes displayed in Figure 1C were further analyzed for overrepresented processes and pathways using KOBAS. Only the top 5 regulated processes are displayed, the numbers of DEGs per pathway is indicated in the brackets.

Inflammatory gene expression also requires the regulated activity of cofactors that are not relevant for cytosolic signaling and rather shape the chromatin compaction or transcription cycles of individual inflammatory target genes [15, 17, 18, 19, 20]. Thus, the lack of effect of SIAH1/2 suppression on the IL-1α-mediated upstream pathways does not pre-clude downstream effects of SIAH1/2 on gene expression. In order to investigate the contribution of SIAH1/2 for the inflammatory transcriptome response, RNA-seq experiments were performed. HeLa cells were treated with specific siRNAs or the adequate scrambled control RNA. After two days, cells were left untreated or stimulated for 4 h with the proinflammatory cytokine IL-1α to trigger gene expression, which was analyzed by RNA-seq experiments. A first data inspection by principal component analysis (PCA) revealed a robust change of gene expression in IL-1α-treated cells (suppl. Figure 2). This experiment identified 490 differentially expressed genes (DEGs) based on a 1.5-fold threshold for regulation between the various conditions (with a FDR <0.05). In unstimulated cells, the knockdown of SIAH1/2 caused gene expression changes in only 11 genes (Figure 1C), indicating no significant effects of these E3 ligases on basal gene expression. The situation was different in IL-1α-stimulated cells, where the knockdown of SIAH1/2 led to the differential expression of 152 genes that were not affected in siScramble-transfected control cells. *Vice versa*, from the 328 DEGs that responded to IL-1α stimulation in the control cells, 61 genes were not regulated after the knockdown of SIAH1/2 (Figure 1C). The percentage of SIAH1/2-coregulated genes may even be underestimated in this experiment, as the knockdown for SIAH1 remained incomplete (see Figure 1A), even after the use of different siRNAs (data not shown). We then performed an enrichment analysis of functional annotations using gene ontology (GO) database. Figure 2 shows the analysis of 266 IL-1α-regulated DEGs that were regulated irrespective from the presence/absence of SIAH1/2. These genes affect processes representing characteristic hallmarks of inflammation including the induction of

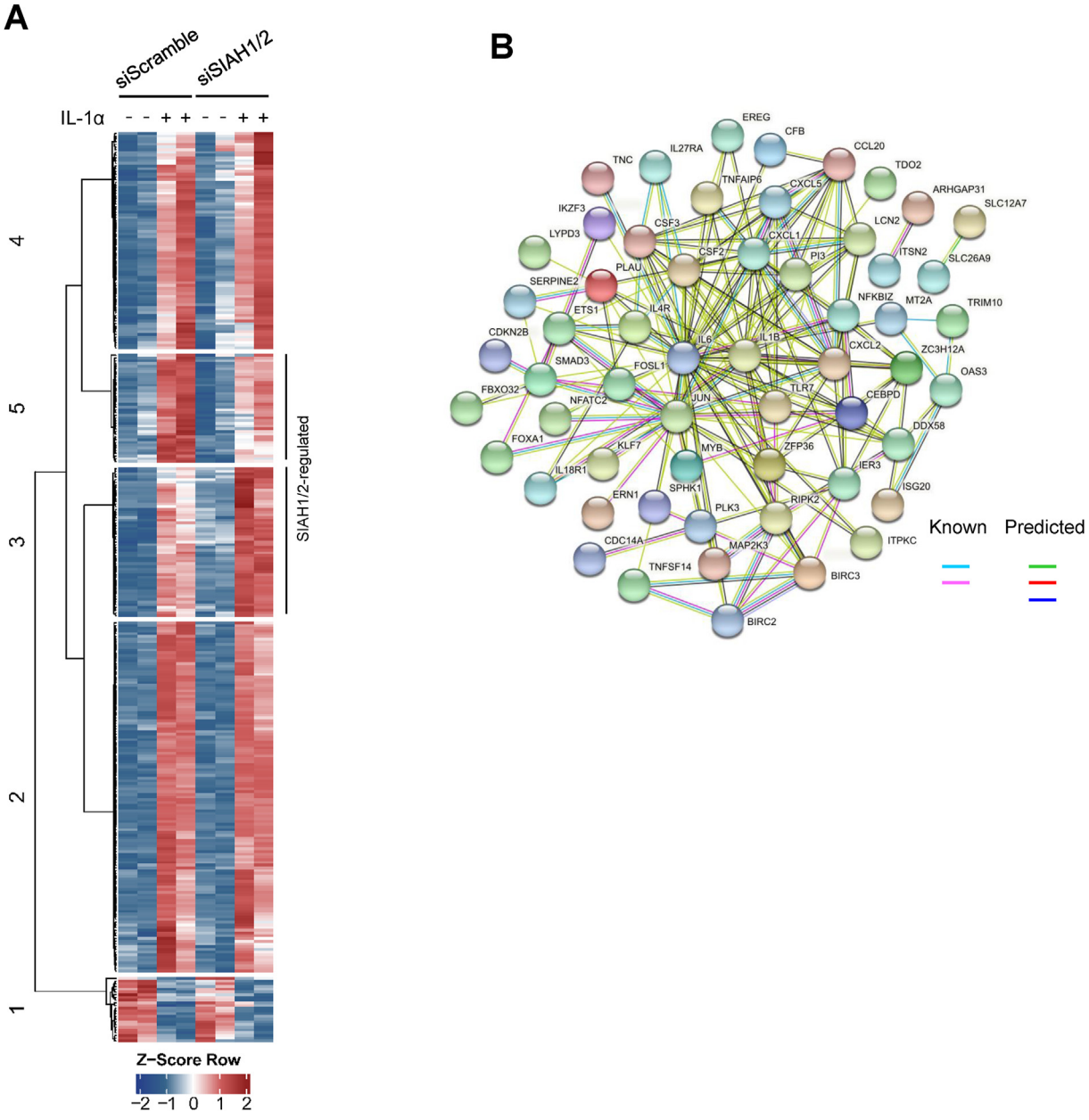

Figure 3. Modulation of IL-1α-regulated gene expression by SIAH1/2. (A) Heat map of K-means clustering of 328 IL-1α-regulated DEGs. (k = 5, Distance metric: Pearson correlation). Counts of all DEGs were transformed by a Z-score normalization per gene. (B) The proteins encoded by gene clusters 3 and 5 were analyzed for known and predicted interactions using the STRING database version 11.0.

NF-κB and MAPK signaling and inducible transcription, as also shown by other transcriptomic analyses of the IL-1α response in epithelial cells [15, 21, 22]. GO analysis of 152 DEGs only regulated after knockdown of SIAH1/2 did not reveal these characteristic processes, similar to the group that showed IL-1α-regulated gene expression only in the presence of both E3 ligases (Figure 2). Almost all of the 328 genes undergoing dynamic IL-1α-dependent regulation were induced by this cytokine (304 genes), while only a small minority were downregulated. We subjected the 328 DEGs responding to IL-1α stimulation in control cells to a K-means clustering analysis. Visualization in a heat map revealed two clusters (cluster 3 and 5) which were co-regulated by SIAH2 (Figure 3A and supplementary Figure 3), while the other DEGs were not significantly affected by the knockdown (supplementary Figure 4). While cluster 3 genes showed increased IL-1α-triggered expression after knockdown of SIAH1/2, cluster 5 genes showed decreased gene expression. Both clusters contain a comparable number of DEGs (cluster 3: 55, cluster 5: 40), implying that SIAH1/2 E3 ubiquitin ligases can be considered as neither pro- nor anti-inflammatory, but rather as general modulators of the amplitude of inflammatory gene expression. Most of the proteins encoded by the genes affected by SIAH1/2 form a physical or regulatory network, based on information deposited in the STRING database [23] and visualized in Figure 3B. The majority of proteins within this network of functional, physical and genetic interactions serve as inflammatory cytokines (including IL-1α and IL-6), signal transducers or transcription factors. The data are also consistent with a model suggesting that SIAH1/SIAH2 do not provide a contribution for upstream signaling cascades or basal gene expression and rather affect IL-1α-regulated gene expression, which is also under the control of several other regulatory circuitries [15, 17, 18, 19]. Consistently, SIAH1 has been frequently identified as an interactor of transcription factors (RUNX1, RARα, KLF10 and STAT3), factors important for posttranscriptional gene regulation and also transcriptional co-regulators such as HIPK2 and the acetyl transferase CBP/p300 [4, 24, 25, 26, 27]. CBP and p300 are important coactivators for proinflammatory transcription factors including NF-κB, AP1 and JAK/STAT [28, 29]. Thus, these coactivators are potentially relevant candidate mediators that can contribute to the observed effects of SIAH1/2 on gene expression. To investigate whether these E3 ligases cooperate to downregulate p300 expression, 293T cells were transiently transfected to express p300 along with SIAH1 and/or SIAH2, followed by analysis of p300 expression by Western blotting (Figure 4A). These experiments revealed efficient reduction of p300 levels by combined expression of SIAH1 and SIAH2, consistent with a cooperative effect of both E3 ligases for the regulation of inflammatory gene expression. This effect could also explain the function of these E3 ligases for the regulation of gene expression, as p300 can be found at the regulatory region of many inflammatory genes [30]. This is exemplified by TNFα-regulated increase of p300 at the promoter regions of the group 3 genes *Birc3* and *Csf2*, as revealed by analysis of publicly available sequence read archive (SRA) data from TNFα-stimulated IMR-90 fibroblasts (Figure 4B). To investigate whether SIAH1 and SIAH2 can also lead to the degradation of chromatin-associated p300, we fused this acetyl transferase to the DNA-binding LacI repressor, thus allowing its specific targeting to arrays of *lacO* (lac operon) sequences that were stably integrated into a heterochromatic region in the genome of U2OS cells (U2OS F6B2). These U2OS F6B2 cells were transfected to express the GFP-LacI-p300 fusion protein (or the GFP-LacI control) either alone or together with SIAH1 or SIAH2. The GFP-LacI and GFP-LacI-p300 fusion proteins were recruited to the integrated *lacO* arrays, as revealed by immunofluorescence analysis (Figure 4C, left). While expression of the GFP-LacI-p300 led to the expected decondensation of heterochromatin, this fusion protein was not detectable in cells coexpressing SIAH1 or SIAH2. The SIAH1/2-mediated degradation did not occur upon expression of the GFP-LacI control protein, revealing that this degradation proceeds via p300, as schematically visualized in Figure 4C. In a reciprocal approach we tested the impact of SIAH1/2 knockdown on GFP-LacI-p300. The downregulation of both E3 ligases led to an expansion of the GFP spots (Figure 4D), consistent with an increased amount/activity of this coactivator. Together, these data suggest that at least a part of the observed effects might be based on the ability of SIAH1/2 to destabilize cofactors such as CBP/p300, but it is reasonable to assume that further and probably unknown targets explain the special relevance of SIAH1/2 for inducible gene expression without affecting basal mRNA levels. It will thus be also interesting to uncover the *in vivo* relevance of this phenotype using inducible double knockout animals in the future.

3. Materials & methods

3.1. Cell culture and transfection

HeLa, 293T and U2OS F6B2 cells haboring stably integrated *lacO* repeats were cultured in DMEM (Life Technologies) supplemented with 10% FCS, 100 U/mL penicillin and 100 μg/mL streptomycin. Medium for U2OS F6B2 cells was complemented with 750 μg/mL G418 (Caymanchem). For knockdown experiments, approximately 60.000 cells/well were seeded in 6-well plates. After reaching 60–70% confluence Lipofectamine transfection with siScramble (10 nM) (D-001810-10-05, Dharmacon) and siRNAs targeting SIAH1 (10 nM) (#4427037, Thermo Fisher) and/or SIAH2 (10 nM) (#L-006561-00-0010, Dharmacon) was carried out for 48 h. One day after transfection in DMEM containing 10% FCS without penicillin/streptomycin, medium was exchanged to full media. The plasmids encoding HA-tagged p300, SIAH1 and SIAH2 [27] and GFP-lacI [31] were described and GFP-lacI-p300 (Addgene ID: 179270) was created. These plasmids were transiently transfected using linear PEI as published [32].

3.2. Immunofluorescence and microscopy

U2OS F6B2 cells were grown in 12-well plates on coverslips. Cells were transfected as displayed in the figure legends. After 24 h cells were washed with PBS and fixed with 3.7% (v/v) formaldehyde for 10 min and further processed as described [31]. Nuclei were stained with Hoechst 33324 (Invitrogen). Cells showing localization of GFP spots at the *lacO* arrays were analyzed using an Nikon microscope (Eclipse TE2000-E). This microscope is further equipped with a coolLED pE-300ultra light source, a Nikon T-RCP controller and a Hamamatsu ORCA SPARK camera. All images were captured with identical microscopy parameters using the Plan Apo 100x Oil Ph3 DM lens. Data were acquired without gamma correction or deconvolution, Z-stacks were recorded (0.75 μm stack size) to include all LacI spots. Images were acquired with NIS Elements 3.00 and processed with Fiji (ImageJ 2.1.0/1.53c). Images were exported as 16-bit uncompressed TIFF with 12-bit depth. Twenty cells were analyzed, representative experiments are shown.

3.3. Western blot and RT-qPCR

Cell extracts were prepared in RIPA lysis buffer as described [33]. Equal amounts of protein contained in cell lysates were separated by SDS-PAGE and used for Western blotting. The following antibodies were purchased from Cell Signaling: p-p65 (S468) (#3039), p-p65 (S536) (#3033), p-IκB-α S32 (#2859), p-IKKα/β (S176/180), p-p38 (T180/Y182) (#9221), p-ERK1/2 (T202/Y204) (#9101), p-cJun (S63) (#9261), p-TBK1 (S172) (#5483). Antibodies recognizing p65 (#sc-8008) and IκBα (#sc-371) were from Santa Cruz Biotechnology, Vinculin (#V9131, Sigma), SIAH1 (#ab2237, Abcam), SIAH2 (#12651-1-AP, Proteintech) and HA (#3F10, Roche) were purchased from the indicated sources. After washing of the membrane and incubation with appropriate horseradish peroxidase-coupled secondary antibodies the signal was detected using the Western Lightning ECL solutions using the ChemiDocTM XRS + System (Bio-Rad Laboratories). Some Western blots were quantitatively analyzed using the ImageJ Lab software version 6.0.1. The RNeasy kit (Qiagen) was used to isolate total RNA. PrimeScript RT Master Mix

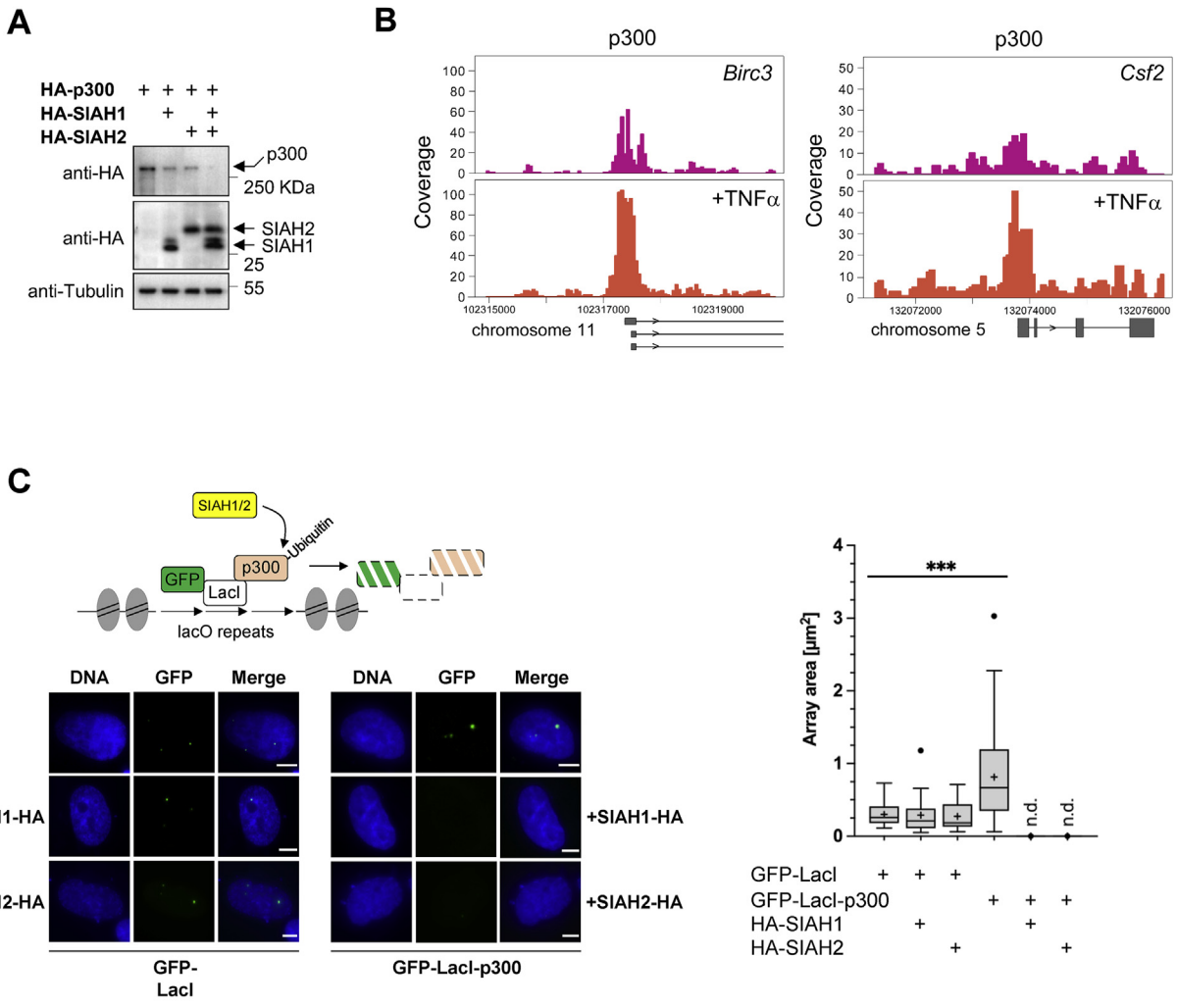

(caption on next page)

Figure 4. Cooperative effect of SIAH1 and SIAH2 on the stability of p300. (A) 293T cells were transfected to express HA-p300 together with SIAH1 and/or SIAH2 as shown. Two days later, cells were lysed and analyzed for expression of the indicated proteins by immunoblotting, a representative experiment is shown. (B) The chromatin binding profiles of p300 from untreated and TNFα-stimulated IMR-90 fibroblasts were downloaded from the SRA database (data sets SRR639057 and SRR639058), coverage profiles for the *Birc3* and *Csf2* promoter regions are shown. The exons are indicated by solid frames and the chromosomal positions are indicated. (C) The *lacO*/LacI system and the SIAH1/2-mediated degradation of the p300 fusion protein is schematically indicated at the top. U2OS F6B2 cells harboring stably integrated *lacO* arrays were transfected to express GFP-LacI or GFP-LacI-p300 fusion proteins. Cells were also transfected with expression plasmids encoding HA-tagged SIAH1 or SIAH2 as shown. After 48 h, cells were fixed, DNA was counterstained with Hoechst 33342 and images were acquired. For each condition, 20 interphase cells were analyzed, representative pictures are shown (scale bar = 5 μm). The areas of the GFP-containing foci were measured with ImageJ, the boxes show the first and third quartile with whiskers extending to the 1.5 interquartile range. The median is denoted by the line in the box, the mean is denoted with a + symbol (n.d. = not determinable). Asterisks indicate *P*-values (***p ≤ 0.001) obtained by two-way ANOVA. (D) U2OS F6B2 cells were transfected with the indicated plasmids and siRNAs. After two days, cells were fixed, nuclear DNA was stained with Hoechst 33342 and the fluorescence emitted by GFP was detected. The quantitative analysis and displays was done as in (C).

(Takara Bio Inc) was used for cDNA synthesis. Generated cDNA was diluted 1:5 using RNase free water. Equal volumes of cDNA were used as a template for amplification by RT-qPCR using the SYBR Green ROX Mix (Thermo) as described [33]. The following primers were used (5′ to 3′): SIAH1-fw: TCAAACATTTTCTGGCCAGTGT; SIAH1-rev: TCATGTGTCTAGCTTCCACCT; SIAH2-fw: CTATGGAGAAGGTGGCCTCG; SIAH2-rev: CGTATGGTGCAGGGTCAGG.

3.4. RNA-seq and data analysis

Libraries for RNA-seq were prepared from 1 μg total RNA with enrichment of polyadenylated RNAs using the VAHTS Stranded mRNA-seq Library Prep Kit (Vazyme, #NR612). Single end sequencing was performed on the NextSeq500 platform using standard Illumina protocols (V2, 75 bp read length, >20 M reads/library). The resulting raw reads were assessed for adapter content, quality and duplication rates with FastQC. Trimmomatic (version 0.39) software was used to trim reads after a quality drop below a mean of Q20 in a window of 10 nucleotides [34]. Reads between 30 and 150 nucleotides were aligned to the reference genome (hg38) using the parameter "–outFilterMismatchNoverLmax 0.1" to increase the maximum ratio of mismatches to mapped length to 10% (Dobin-STAR) The featureCounts 1.6.5 tool from the Subread package [35] was used to count the number of reads aligning to genes. Reads overlapping multiple genes or aligning to multiple regions were excluded and only reads mapping at least partially to exons were used for aggregation. Differential gene expression was computed using DESeq2 (1.26.0), with standard parameters. For differential expression we only considered genes with ≥5 reads, a maximum Benjamini-Hochberg corrected *P*-value of 0.05 and a fold change ≥ ± 1.5 (log2 = ± 0.585). The R packages FactoMineR and factoextra were used for dimension reduction analyses (PCA) using the DESeq2 normalized and regularized log transformed counts. Gene set enrichment analyses of DEGs were performed with KOBAS [36]. Pathways with Benjamini-Hochberg corrected *P*-Value < 0.05 (represented by dashed line) were displayed as barplots. Heatmaps were produced by R (Package complexheatmap) to show DEG regulation per contrast. Counts of all DEGs were transformed by a Z-score normalization per row for heatmap assembly.

To visualize p300 occupancy at promoters and regulatory regions controlling the expression of SIAH1/2-dependent genes, raw data deposited in the SRA data base were downloaded via Galaxy with fasterq-dump and mapped using bowtie2 (2.4.2) against hg38 (default settings). Coverage tracks were created with deepTools (multiBigWigSummary 3.5.1) and graphs were created with R and a version of Trackplot.R (https://github.com/PoisonAlien/trackplot).

Declarations

Author contribution statement

M. Lienhard Schmitz: Conceived and designed the experiments; Analyzed and interpreted the data.

Jan Dreute, Maximilian Pfisterer, Stefan Günther: Performed the experiments; Analyzed and interpreted the data.

Michael Kracht: Analyzed and interpreted the data.

Shashipavan Chillappagari: Performed the experiments; Analyzed and interpreted the data; Wrote the paper.

Funding statement

This work was supported by the Deutsche Forschungsgemeinschaft (DFG, German Research Foundation): TRR81/3 (A07 to MLS; B02 to MK; project 109546710); SFB1213 (B03 to MK and MLS; project 268555672); SFB1021 (C01 to MLS; C02 to MK; Z03 to MK; project 197785619); and GRK 2573 (RP4 to MLS; RP5 to MK; project 416910386). Work in the laboratory of LS is supported by the IMPRS program of the Max Planck Society.

Data availability statement

Data associated with this study has been deposited at the GEO repository under the accession number GSE179190.

Declaration of interests statement

The authors declare no conflict of interest.

Additional information

Supplementary content related to this article has been published online at https://doi.org/10.1016/j.heliyon.2022.e09029.

Acknowledgements

We thank Yvonne Horn and Markus Schwinn for their excellent technical assistance.

References

[1] I.J. Pepper, R.E. Van Sciver, A.H. Tang, Phylogenetic analysis of the SINA/SIAH ubiquitin E3 ligase family in Metazoa, BMC Evol. Biol. 17 (1) (2017) 182.

[2] J.T. Lee, T.C. Wheeler, L. Li, L.S. Chin, Ubiquitination of alpha-synuclein by Siah-1 promotes alpha-synuclein aggregation and apoptotic cell death, Hum. Mol. Genet. 17 (6) (2008) 906–917.

[3] I.J. Frew, V.E. Hammond, R.A. Dickins, J.M. Quinn, C.R. Walkley, N.A. Sims, R. Schnall, N.G. Della, A.J. Holloway, M.R. Digby, P.W. Janes, D.M. Tarlinton, L.E. Purton, M.T. Gillespie, D.D. Bowtell, Generation and analysis of Siah2 mutant mice, Mol. Cell Biol. 23 (24) (2003) 9150–9161.

[4] M.A. Calzado, L. de la Vega, A. Moller, D.D. Bowtell, M.L. Schmitz, An inducible autoregulatory loop between HIPK2 and Siah2 at the apex of the hypoxic response, Nat. Cell Biol. 11 (1) (2009) 85–91.

[5] H. Habelhah, A. Laine, H. Erdjument-Bromage, P. Tempst, M.E. Gershwin, D.D. Bowtell, Z. Ronai, Regulation of 2-oxoglutarate (alpha-ketoglutarate) dehydrogenase stability by the RING finger ubiquitin ligase Siah, J. Biol. Chem. 279 (51) (2004) 53782–53788.

[6] K. Nakayama, I.J. Frew, M. Hagensen, M. Skals, H. Habelhah, A. Bhoumik, T. Kadoya, H. Erdjument-Bromage, P. Tempst, P.B. Frappell, D.D. Bowtell, Z. Ronai, Siah2 regulates stability of prolyl-hydroxylases, controls HIF1alpha abundance, and modulates physiological responses to hypoxia, Cell 117 (7) (2004) 941–952. S0092867404005410 [pii].

[7] C.H. Nagel, N. Albrecht, K. Milovic-Holm, L. Mariyanna, B. Keyser, B. Abel, B. Weseloh, T.G. Hofmann, M.M. Eibl, J. Hauber, Herpes simplex virus immediate-

early protein ICP0 is targeted by SIAH-1 for proteasomal degradation, J. Virol. 85 (15) (2011) 7644–7657.
[8] B. Aslam, J. Ahmad, A. Ali, R.Z. Paracha, S.H. Tareen, S. Khusro, T. Ahmad, S.A. Muhammad, U. Niazi, V. Azevedo, Structural modeling and analysis of dengue-mediated inhibition of interferon signaling pathway, Genet. Mol. Res. 14 (2) (2015) 4215–4237.
[9] S. Yeom, S.S. Kim, H. Jeong, K.L. Jang, Hepatitis B virus X protein activates E3 ubiquitin ligase Siah-1 to control virus propagation via a negative feedback loop, J. Gen. Virol. 98 (7) (2017) 1774–1784.
[10] J. Wang, K. Huo, L. Ma, L. Tang, D. Li, X. Huang, Y. Yuan, C. Li, W. Wang, W. Guan, H. Chen, C. Jin, J. Wei, W. Zhang, Y. Yang, Q. Liu, Y. Zhou, C. Zhang, Z. Wu, W. Xu, Y. Zhang, T. Liu, D. Yu, Y. Zhang, L. Chen, D. Zhu, X. Zhong, L. Kang, X. Gan, X. Yu, Q. Ma, J. Yan, L. Zhou, Z. Liu, Y. Zhu, T. Zhou, F. He, X. Yang, Toward an understanding of the protein interaction network of the human liver, Mol. Syst. Biol. 13 (12) (2017) 965.
[11] J.B. Garrison, R.G. Correa, M. Gerlic, K.W. Yip, A. Krieg, C.M. Tamble, R. Shi, K. Welsh, S. Duggineni, Z. Huang, K. Ren, C. Du, J.C. Reed, ARTS and Siah collaborate in a pathway for XIAP degradation, Mol. Cell 41 (1) (2011) 107–116.
[12] J. Woodsmith, R.C. Jenn, C.M. Sanderson, Systematic analysis of dimeric E3-RING interactions reveals increased combinatorial complexity in human ubiquitination networks, Mol. Cell. Proteomics 11 (7) (2012). M111 016162.
[13] G. Polekhina, C.M. House, N. Traficante, J.P. Mackay, F. Relaix, D.A. Sassoon, M.W. Parker, D.D. Bowtell, Siah ubiquitin ligase is structurally related to TRAF and modulates TNF-alpha signaling, Nat. Struct. Biol. 9 (1) (2002) 68–75.
[14] S. Bacher, J. Meier-Soelch, M. Kracht, M.L. Schmitz, Regulation of transcription factor NF-kappaB in its natural habitat: the nucleus, Cells 10 (4) (2021).
[15] S.S. Weiterer, J. Meier-Soelch, T. Georgomanolis, A. Mizi, A. Beyerlein, H. Weiser, L. Brant, C. Mayr-Buro, L. Jurida, K. Beuerlein, H. Muller, A. Weber, U. Tenekeci, O. Dittrich-Breiholz, M. Bartkuhn, A. Nist, T. Stiewe, I.W.F. van, T. Riedlinger, M.L. Schmitz, A. Papantonis, M. Kracht, Distinct IL-1alpha-responsive enhancers promote acute and coordinated changes in chromatin topology in a hierarchical manner, EMBO J. 39 (1) (2020), e101533.
[16] E. Santelli, M. Leone, C. Li, T. Fukushima, N.E. Preece, A.J. Olson, K.R. Ely, J.C. Reed, M. Pellecchia, R.C. Liddington, S. Matsuzawa, Structural analysis of Siah1-Siah-interacting protein interactions and insights into the assembly of an E3 ligase multiprotein complex, J. Biol. Chem. 280 (40) (2005) 34278–34287.
[17] K. Handschick, K. Beuerlein, L. Jurida, M. Bartkuhn, H. Muller, J. Soelch, A. Weber, O. Dittrich-Breiholz, H. Schneider, M. Scharfe, M. Jarek, J. Stellzig, M.L. Schmitz, M. Kracht, Cyclin-dependent kinase 6 is a chromatin-bound cofactor for NF-kappaB-dependent gene expression, Mol.Cell 53 (2) (2014) 193–208. S1097-2765(13)00870-8 [pii].
[18] M.J. Barter, K. Cheung, J. Falk, A.C. Panagiotopoulos, C. Cosimini, S. O'Brien, K. Teja-Putri, G. Neill, D.J. Deehan, D.A. Young, Dynamic chromatin accessibility landscape changes following interleukin-1 stimulation, Epigenetics 16 (1) (2021) 106–119.
[19] J.D. Brown, C.Y. Lin, Q. Duan, G. Griffin, A. Federation, R.M. Paranal, S. Bair, G. Newton, A. Lichtman, A. Kung, T. Yang, H. Wang, F.W. Luscinskas, K. Croce, J.E. Bradner, J. Plutzky, NF-kappaB directs dynamic super enhancer formation in inflammation and atherogenesis, Mol. Cell 56 (2) (2014) 219–231.
[20] J. Meier-Soelch, L. Jurida, A. Weber, D. Newel, J. Kim, T. Braun, M.L. Schmitz, M. Kracht, RNAi-based identification of gene-specific nuclear cofactor networks regulating interleukin-1 target genes, Front. Immunol. 9 (2018) 775.
[21] M. Poppe, S. Wittig, L. Jurida, M. Bartkuhn, J. Wilhelm, H. Muller, K. Beuerlein, N. Karl, S. Bhuju, J. Ziebuhr, M.L. Schmitz, M. Kracht, The NF-kappaB-dependent and -independent transcriptome and chromatin landscapes of human coronavirus 229E-infected cells, PLoS Pathog. 13 (3) (2017), e1006286.
[22] E. Ziesché, D. Kettner-Buhrow, A. Weber, T. Wittwer, L. Jurida, J. Soelch, H. Muller, D. Newel, P. Kronich, H. Schneider, O. Dittrich-Breiholz, S. Bhaskara, S.W. Hiebert, M.O. Hottiger, H. Li, E. Burstein, M.L. Schmitz, M. Kracht, The coactivator role of histone deacetylase 3 in IL-1-signaling involves deacetylation of p65 NF-kappaB, Nucleic Acids Res. 41 (1) (2013) 90–109, gks916 [pii].
[23] D. Szklarczyk, A.L. Gable, K.C. Nastou, D. Lyon, R. Kirsch, S. Pyysalo, N.T. Doncheva, M. Legeay, T. Fang, P. Bork, L.J. Jensen, C. von Mering, The STRING database in 2021: customizable protein-protein networks, and functional characterization of user-uploaded gene/measurement sets, Nucleic Acids Res. 49 (D1) (2021) D605–D612.
[24] O.H. Krämer, S. Muller, M. Buchwald, S. Reichardt, T. Heinzel, Mechanism for ubiquitylation of the leukemia fusion proteins AML1-ETO and PML-RARalpha, Faseb. J. 22 (5) (2008) 1369–1379.
[25] S.A. Johnsen, M. Subramaniam, D.G. Monroe, R. Janknecht, T.C. Spelsberg, Modulation of transforming growth factor beta (TGFbeta)/Smad transcriptional responses through targeted degradation of TGFbeta-inducible early gene-1 by human seven in absentia homologue, J. Biol. Chem. 277 (34) (2002) 30754–30759.
[26] M. Shin, E.H. Yi, B.H. Kim, J.C. Shin, J.Y. Park, C.H. Cho, J.W. Park, K.Y. Choi, S.K. Ye, STAT3 potentiates SIAH-1 mediated proteasomal degradation of beta-catenin in human embryonic kidney cells, Mol. Cell 39 (11) (2016) 821–826.
[27] I. Grishina, K. Debus, C. Garcia-Limones, C. Schneider, A. Shresta, C. Garcia, M.A. Calzado, M.L. Schmitz, SIAH-mediated ubiquitination and degradation of acetyl-transferases regulate the p53 response and protein acetylation, Biochim. Biophys. Acta 1823 (12) (2012) 2287–2296. S0167-4889(12)00280-7 [pii].
[28] M.E. Gerritsen, A.J. Williams, A.S. Neish, S. Moore, Y. Shi, T. Collins, CREB-binding protein/p300 are transcriptional coactivators of p65, Proc. Natl. Acad. Sci. U. S. A. 94 (7) (1997) 2927–2932.
[29] A.E. Horvai, L. Xu, E. Korzus, G. Brard, D. Kalafus, T.M. Mullen, D.W. Rose, M.G. Rosenfeld, C.K. Glass, Nuclear integration of JAK/STAT and Ras/AP-1 signaling by CBP and p300, Proc. Natl. Acad. Sci. U. S. A. 94 (4) (1997) 1074–1079.
[30] W. Vanden Berghe, K. De Bosscher, E. Boone, S. Plaisance, G. Haegeman, The nuclear factor-kappaB engages CBP/p300 and histone acetyltransferase activity for transcriptional activation of the interleukin-6 gene promoter, J. Biol. Chem. 274 (45) (1999) 32091–32098.
[31] J. Haas, D. Bloesel, S. Bacher, M. Kracht, M.L. Schmitz, Chromatin targeting of HIPK2 leads to acetylation-dependent chromatin decondensation, Front. Cell Dev. Biol. 8 (2020) 852.
[32] S. Bacher, H. Stekman, C.M. Farah, A. Karger, M. Kracht, M.L. Schmitz, MEKK1-Dependent activation of the CRL4 complex is important for DNA damage-induced degradation of p21 and DDB2 and cell survival, Mol. Cell Biol. 41 (10) (2021), e0008121.
[33] S. Chillappagari, R. Belapurkar, A. Moller, N. Molenda, M. Kracht, S. Rohrbach, M.L. Schmitz, SIAH2-mediated and organ-specific restriction of HO-1 expression by a dual mechanism, Sci. Rep. 10 (1) (2020) 2268.
[34] A.M. Bolger, M. Lohse, B. Usadel, Trimmomatic: a flexible trimmer for Illumina sequence data, Bioinformatics 30 (15) (2014) 2114–2120.
[35] Y. Liao, G.K. Smyth, W. Shi, featureCounts: an efficient general purpose program for assigning sequence reads to genomic features, Bioinformatics 30 (7) (2014) 923–930.
[36] C. Xie, X. Mao, J. Huang, Y. Ding, J. Wu, S. Dong, L. Kong, G. Gao, C.Y. Li, L. Wei, KOBAS 2.0: a web server for annotation and identification of enriched pathways and diseases, Nucleic Acids Res. 39 (2011) W316–W322. Web Server issue.